SEMARAK ILMU PUBLISHING

CFD Letters

Journal homepage:
https://semarakilmu.com.my/journals/index.php/CFD_Letters/index
ISSN: 2180-1363

Effect of Catheter and Stenosis on Solute Diffusion in Non-Newtonian Blood Flow through a Catheterized Stenosed Artery

Intan Diyana Munir[1], Nurul Aini Jaafar[1,*], Sharidan Shafie[1]

[1] Department of Mathematical Sciences, Faculty of Science, Universiti Teknologi Malaysia, 81310 Johor Bahru, Johor, Malaysia

ARTICLE INFO

Article history:
Received 6 September 2022
Received in revised form 28 September 2022
Accepted 20 October 2022
Available online 30 November 2022

Keywords:
Steady blood flow; Unsteady solute dispersion; Herschel-Bulkley model; Generalized Dispersion Model; Catheterized stenosed artery.

ABSTRACT

The presence of stenosis at the wall of the artery lead to further cardiovascular diseases such as heart attack, stroke and many more. Treatment of a stenosed artery includes the insertion of a catheter through the artery which affects the blood flow and solute dispersion. This present study focuses on the effect of catheter radius and stenosis height on the blood flow and solute dispersion behavior. The problem is modelled using the Herschel-Bulkley fluid to represent the blood rheology, with catheter and stenosis as the boundary conditions. Analytical solutions in integral form are obtained by solving the momentum equation and Herschel-Bulkley constitutive equation. The integrals are numerically evaluated using the Simpson's 3/8 rule and Regula-Falsi method to obtain the blood velocity. The obtained velocity is employed into the unsteady convective-diffusion equation and solved using the generalized dispersion model (GDM) to analyse the behaviour of solute diffusion. The influence of catheter radius and stenosis height on the diffusion coefficient and mean concentration of solute are observed. Results show that the diffusion coefficient decreases as the catheter radius and stenosis height increases. A decrease in diffusion coefficient simultaneously increases the solute mean concentration.

1. Introduction

Atherosclerosis is a medical condition caused by the accumulation of fats, cholesterol and other materials at the lining of the arterial wall. This condition can lead to the thickening of the arterial wall, narrowing of the lumen and obstruction of blood flow [1]. One of the many treatments of a stenosed artery is through the catheterization of the stenosed artery to either deliver drug or open up the narrowed artery by placing a stent at the stenosed site. Introducing a catheter into an artery poses various risk of complications that includes cardiac perforation, heart arrhythmias, stroke, blood loss and several more [2]. Thus, extra measures should be considered by doctors before performing the treatment. Research on solute dispersion through a catheterized stenosed artery can contribute and improve the biomedical field related to catheterization of a stenosed artery.

Study of solute dispersion is significant as the behaviour of drug solute within the artery could affect the effectiveness of the drug. Debnath *et al.,* [3] analysed the unsteady dispersion using the

* *Corresponding author.*
E-mail address: nurulaini.jaafar@utm.my (Nurul Aini Jaafar)

https://doi.org/10.37934/cfdl.14.12.1126

Casson fluid to model the blood flowing through an artery with the presence of catheter. They utilized the Aris-Barton method in solving for the dispersion coefficient and Hermite polynomial to solve for the axial mean concentration. In comparison with the GDM method, the GDM method is more practical. This is because the solution expressions provided by Gill and Sankarasubramanian [4] harbours the high order parameter of concentration rate. Thus, it can provide more details on the dispersion mechanism such as dispersion function, convection coefficient, diffusion coefficient and mean concentration. Sebastian and Nagarani [5] studied the unsteady dispersion of solute through an annulus with wall absorption present. They used the GDM method to obtain the expression of the convection and diffusion coefficients. Nagarani *et al.,* [6] investigated the influence of boundary absorption on the dispersion of solute through a catheterized artery and utilizes the GDM to solve for the dispersion function solution. Nagarani and Sebastian [7] observed the dispersion behaviour affected by the flow unsteadiness through an annulus and adopted the GDM method to solve for the diffusion coefficient and mean concentration. Abidin *et al.,* [1] conducted a research on the unsteady solute dispersion of Bingham flow through an artery with overlapping stenosis. They utilized the GDM method to solve for the steady and unsteady dispersion functions of solute. Based on the literatures, it is appropriate to say that the GDM method is a practical and pragmatic approach in solving the expression of solute dispersion such as dispersion function, diffusion coefficient and mean concentration.

One of the fluid popular in studying the of solutes convection and diffusion is the nanofluid. In choosing the suitable fluid model to represent the blood rheology, no particular model is collectively acknowledged to reflect the blood viscosity exact nature [8]. Therefore, researchers have used Newtonian and various non-Newtonian models in representing the blood flow. The type of model chosen depends on the problems of the artery. For instance, this present study focuses on the blood flowing through a catheterized stenosed artery. Therefore, the model chosen should be able to explain the flow in a vastly narrow artery. The model suiQ for this present study is the Herschel-Bulkley model because it is suitable to be utilized at low shear rate flow in very narrow arteries where the yield stress is high [9]. Furthermore, the yield stress and power-law index parameters are harboured by the Herschel-Bulkley model [10]. The Herschel-Bulkley model can also be modified into other models such as Newtonian, Power-Law and Bingham models which gives an additional advantage over other type of non-Newtonian models [11]. Sankar and Hemalatha [12] observed the blood flowing through an artery using the Herschel-Bulkley model with the presence of catheter. Sankar and Lee [13] studied the behaviour of blood flow in a two-fluid artery with the presence of catheter by utilizing the Herschel-Bulkley model to represent the blood. Neeraja *et al.,* [14] used the Herschel-Bulkley model in their research on the blood flow through a stenosed blood vessel. Abbas *et al.,* [15] analysed the blood flow by utilizing the Herschel-Bulkley model through an artery with multiple stenosis present at the arterial wall. Srivastava and Rastogi [16] observed blood flow through a catheterized artery using the Herschel-Bulkley model affected by the hematocrit and stenosis shape. Gudekote *et al.,* [17] utilized the Herschel-Bulkley model in their study of peristaltic blood flow through an elastic tube with the presence of porous wall slip due to the model's validity for lower shear rate values. Jaafar *et al.,* [18] studied the unsteady solute dispersion with the presence of chemical reaction through a stenosed artery by using the Herschel-Bulkley model in representing the blood and adopting the GDM method in solving for the steady and unsteady dispersion functions. All the literature mentioned uses the Herschel-Bulkley model in depicting the blood flow. However, most of the studies that uses the Herschel-Bulkley model to portray the blood behaviour only focuses on the blood flow analysis and neglects the aspect of solute dispersion. Moreover, the research of solute dispersion in a blood flow using the Herschel-Bulkley model through a very narrow artery due to both catheter and stenosis simultaneously present has not yet been explored. Therefore, the objective of

the present research is to investigate the influence of catheter radius and stenosis height on the diffusion coefficient and mean concentration modelled by the Herschel-Bulkley model. The result of this present study could potentially advance the medical field such as refining the arterial catheterization procedure, making better medical device and refining drug prescribing related to stenosed artery.

2. Methodology

2.1 Problem Formulation

The solute dispersion in terms of diffusion coefficient and mean concentration in a blood flowing through a catheterized artery with stenosis present at the arterial wall is considered. The blood flow is considered as a steady, fully-developed, laminar Herschel-Bulkley model through an artery with the presence of catheter of radius $\bar{R}$. Figure 1 depicts the problem configuration of the blood flowing through the catheterized artery where $\bar{r}$ is the radius, $\bar{z}$ is the axial direction of the flow, k is the dimensionless catheter radius, λ_1 is the plane location of the lower part of plug flow region, λ_2 is the plane location of the upper part of plug flow region, $\bar{\delta}$ is the height of stenosis, $\bar{l}_0$ is the length of stenosis and $\bar{R}(\bar{z})$ is the stenosed artery flow region radius. There are outer flow and plug flow regions between the wall of the catheter and the artery. The outer flow region is further distinguished into bottom and top region because the fluid velocities in those two regions are different as shown in Figure 1. The radiuses of these three regions are $k<\bar{r}<\lambda_1$ for the bottom outer flow region, $\lambda_1<\bar{r}<\lambda_2$ for the plug flow region and $\lambda_2<\bar{r}<\bar{R}$ for the top outer flow region. Formulation and mathematical solving in this present study utilizes the cylindrical polar coordinates.

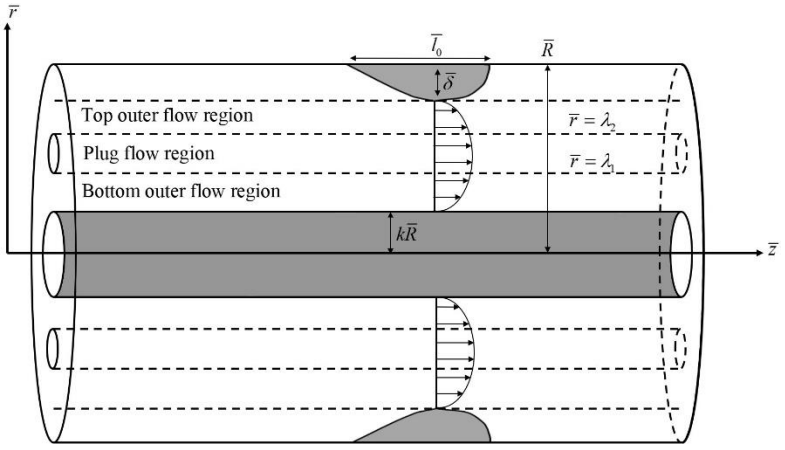

Fig. 1. The configuration of blood flowing through a catheterized stenosed artery

The continuity and momentum equation in the cylindrical coordinate given by Tey *et al.,* [19] is adapted to the present study problem. This present study focuses on the solute dispersion through the axial flow of Herschel-Bulkley model in the $\bar{z}$ direction. Thus, the azimuthal and radial direction velocities are neglected and assumed to be zero. The flow is uniform and the velocity is independent from the radial and azimuthal directions due to axial symmetry. The continuity, momentum and Herschel-Bulkley constitutive equations for the steady flow in the $\bar{z}$ direction and cylindrical coordinate can be governed as given below:

$$\frac{\partial \bar{w}}{\partial \bar{z}} = 0, \tag{1}$$

$$\frac{d\bar{p}}{d\bar{z}} = -\frac{1}{\bar{r}}\frac{d}{d\bar{r}}(\bar{r}\bar{\tau}), \qquad k\bar{R} \le \bar{r} \le \bar{R} \tag{2}$$

and

$$\begin{aligned} |\bar{\tau}| &= \bar{\mu}_H^{1/n}\left(-\frac{\partial \bar{w}}{\partial \bar{r}}\right)^{1/n} + \bar{\tau}_y \quad \text{if} \quad |\bar{\tau}| \ge \bar{\tau}_y, \\ \frac{\partial \bar{w}}{\partial \bar{r}} &= 0 \quad \text{if} \quad |\bar{\tau}| < \bar{\tau}_y, \end{aligned} \tag{3}$$

where $\bar{w}$ is the velocity in the $\bar{z}$ direction, $\bar{p}$ is the pressure, $\bar{\tau}$ is the shear stress, $\bar{\mu}_H$ is the viscosity of Herschel-Bulkley fluid, n is the power-law index and τ_y is the yield stress,. The pressure gradient $d\bar{p}/d\bar{z}$ in the momentum equation is measured as a fixed value. The momentum equation boundary condition is given as

$$\begin{aligned} \bar{\tau} &= -\bar{\tau}_y \quad \text{at} \quad \bar{r} = \lambda_1, \\ \bar{\tau} &= \bar{\tau}_y \quad \text{at} \quad \bar{r} = \lambda_2. \end{aligned} \tag{4}$$

The Herschel-Bulkley constitutive equation in Eq. (3) can be written as

$$\bar{\mu}_H\left(\frac{\partial \bar{w}}{\partial \bar{r}}\right) = -\left(|\bar{\tau}| - \bar{\tau}_y\right)^n \quad \text{if} \quad |\bar{\tau}| \ge \bar{\tau}_y, \tag{5}$$

with the boundary conditions of

$$\begin{aligned} \bar{w} &= 0 \quad \text{at} \quad \bar{r} = k\bar{R}, \\ \bar{w} &= 0 \quad \text{at} \quad \bar{r} = \bar{R}(\bar{z}), \end{aligned} \tag{6}$$

where $\bar{R}(\bar{z})$ is defined as

$$\bar{R}(\bar{z}) = \begin{cases} \bar{R} & \text{otherwise,} \\ \bar{R} - \dfrac{\bar{\delta}}{2}\left[1 + \cos\left(\dfrac{2\pi}{\bar{l}_0}\left(\bar{z} - \bar{d} - \dfrac{\bar{l}_0}{2}\right)\right)\right] & \text{when} \quad \bar{d} \le \bar{z} \le \bar{l}_0 + \bar{d}, \end{cases} \tag{7}$$

where $\bar{\delta}$ is stenosis height, $\bar{l}_0$ is stenosis length and $\bar{d}$ is stenosis location. The solute dispersion equation in a simplified form is given by the unsteady convective-diffusion equation as

$$\frac{\partial \bar{C}}{\partial \bar{t}} + \bar{w}\frac{\partial \bar{C}}{\partial \bar{z}} = \bar{D}_m\left(\frac{1}{\bar{r}}\frac{\partial}{\partial \bar{r}}\left(\bar{r}\frac{\partial}{\partial \bar{r}}\right) + \frac{\partial^2}{\partial \bar{z}^2}\right)\bar{C}, \tag{8}$$

where $\bar{C}$ is the concentration of solute, $\bar{t}$ is the time and $\bar{D}_m$ is the diffusivity of molecules. The unsteady convective-diffusion equation in Eq. (8) has the initial and boundary conditions of

$$\bar{C}(\bar{r},\bar{z},0)=\bar{C}_0 \quad \text{if} \quad |\bar{z}|\le \bar{z}_s/2,$$
$$\bar{C}(\bar{r},\bar{z},0)=0 \quad \text{if} \quad |\bar{z}|> \bar{z}_s/2, \tag{9}$$

$$\bar{C}(\bar{r},\infty,\bar{t})=0 \tag{10}$$

and

$$\frac{\partial \bar{C}}{\partial \bar{r}}(k,\bar{z},\bar{t})=\frac{\partial \bar{C}}{\partial \bar{r}}(\bar{R}(\bar{z}),\bar{z},\bar{t})=0, \tag{11}$$

where $\bar{C}_0$ is the reference solute concentration and z_s is the length of solute.

2.2 Solution for Flow Velocity

In solving for the blood flow velocity, Eqs. (1), (2) and (5) are first non-dimensionalized by utilizing the following non-dimensional variables introduced as follows:

$$w=\frac{\bar{w}}{\bar{w}_0}, r=\frac{\bar{r}}{\bar{R}}, z=\frac{\bar{z}}{\bar{R}}, \tau=\frac{2\bar{\tau}}{\bar{p}_0\bar{R}}, C=\frac{\bar{C}}{\bar{C}_0}, t=\frac{\bar{D}_m\bar{t}}{\bar{R}^2}, R(z)=\frac{\bar{R}(\bar{z})}{\bar{R}}, d=\frac{\bar{d}}{\bar{R}}, l_0=\frac{\bar{l}_0}{\bar{R}}, \delta=\frac{\bar{\delta}}{\bar{R}}, \tag{12}$$

where w, r, z, τ, C, t, $R(z)$, d, l_0 and δ are the non-dimensional variables of velocity, radius, axial coordinate, shear stress, concentration, time, stenosis size, stenosis location, stenosis length and stenosis height respectively and $\bar{p}_0$ is the absolute magnitude of typical pressure gradient. The pressure gradient can be written as $d\bar{p}/d\bar{z}=-\bar{p}_0 p_s$ where p_s is the static pressure gradient. The viscosity $\bar{\mu}$ is $\bar{\mu}=\bar{\mu}_H\left(2/\bar{p}_0\bar{R}\right)^{m-1}$ has the Newtonian fluid's viscosity dimension. The dimensionless form of momentum and Herschel-Bulkley constitutive equations are obtained as

$$2p_s=\frac{1}{r}\frac{d}{dr}(r\tau), \quad k\le r\le 1, \tag{13}$$

$$\left(\frac{\partial w}{\partial r}\right)=-\left(|\tau|-\tau_y\right)^n. \tag{14}$$

Eq. (13) is solved for τ through integration with respect to r to obtain

$$\tau=\frac{p_s}{r}(r^2-\lambda^2), \tag{15}$$

where $\lambda^2=\lambda_1\lambda_2$. The dimensionless τ in Eq. (15) is then substituted into Eq. (14) and solved for w in the bottom outer flow region, plug flow region and top outer flow region expressed respectively as

$$w_o^+ = -p_s^n \left(\int_k^r \left(\frac{\lambda^2 - r^2}{r} \right)^n dr - m\theta \int_k^r \left(\frac{\lambda^2 - r^2}{r} \right)^{n-1} dr \right), \text{ for } k \le r \le \lambda_1,$$
$$w_p = \text{constant} \text{ for } \lambda_1 \le r \le \lambda_2, \tag{16}$$
$$w_o^{++} = -p_s^n \left(\int_r^{R(z)} \left(\frac{r^2 - \lambda^2}{r} \right)^n dr - m\theta \int_r^{R(z)} \left(\frac{r^2 - \lambda^2}{r} \right)^{n-1} dr \right), \text{ for } \lambda_2 \le r \le R(z),$$

where $\theta = \tau_y / p_s$. The integral terms in Eq. (16) are numerically solved by utilizing the Simpson's 3/8 rule. Due to the velocity distribution throughout the blood flow region having a continuity condition, the equation of $w_o^+ (r = \lambda_1) = w_p = w_o^{++} (r = \lambda_2)$ is obtained and used to find the value of λ_1 and λ_2 using the Regula-Falsi method.

2.3 Solution for Diffusion Coefficient

The dimensionless variables in Eq. (12) are substituted into the unsteady convective-diffusion equation in Eq. (8) and the dimensionless unsteady convective-diffusion equation is written as

$$\frac{\partial C}{\partial t} + w \frac{\partial C}{\partial z} = \left(\frac{1}{r} \frac{\partial}{\partial r} \left(r \frac{\partial}{\partial r} \right) + \frac{1}{Pe^2} \frac{\partial^2}{\partial z^2} \right) C, \tag{17}$$

where $Pe = \bar{R}\bar{w}_0 / \bar{D}_m$. The dimensionless initial and boundary conditions of Eqs. (9), (10) and (11) are

$$C(r, z, 0) = 1 \text{ if } |z| \le z_s/2,$$
$$C(r, z, 0) = 0 \text{ if } |z| > z_s/2, \tag{18}$$
$$C(r, \infty, t) = 0 \tag{19}$$

and

$$\frac{\partial C}{\partial r}(k, z, t) = \frac{\partial C}{\partial r}(R(z), z, t) = 0 \tag{20}$$

respectively. The solute convection is assumed to be moving across the artery with the average fluid velocity w_m given by the expression of

$$w_m = \frac{2}{R(z)^2 - k^2} \int_k^{R(z)} wr \; dr. \tag{21}$$

A new coordinate system (r, z_1, t) is defined with a new axial coordinate z_1 where $z_1 = z - u_m t$ for solving the solute concentration. Following Gill and Sankarasubramanian [4], Eq. (17) is assumed to be in a series expansion solution of

$$C(r,z,t) = C_m(z,t) + \sum_{j=1}^{\infty} f_j\,(r,t)\frac{\partial^j C_m(z,t)}{\partial z_1^j}, \tag{22}$$

where C_m is the cross-sectional mean solute concentration defined by

$$C_m(z,t) = \frac{2}{R(z)^2 - k^2}\int_k^{R(z)} C(r,z,t) r\ dr \tag{23}$$

and f_j is the dispersion function. The unsteady convective-diffusion equation is transformed into a coordinate system of (r, z_1, t) by substituting the definition of z_1 into Eq. (17). Eq. (22) is then substituted into the transformed unsteady convective-diffusion equation to obtain

$$\begin{aligned}&\frac{\partial C_m}{\partial t} + (w - w_m)\frac{\partial C_m}{\partial z_1} - \frac{1}{Pe^2}\frac{\partial^2 C_m}{\partial z_1^2}\\ &+\sum_{j=1}^{\infty}\left[\left(\frac{\partial f_j}{\partial t} - L^2 f_j\right)\frac{\partial^j C_m}{\partial z_1^j} + (w - w_m) f_j \frac{\partial^{j+1} C_m}{\partial z_1^{j+1}} - \frac{1}{Pe^2} f_j \frac{\partial^{j+2} C_m}{\partial z_1^{j+2}} + f_j \frac{\partial^{j+1} C_m}{\partial t \partial z_1^j}\right] = 0.\end{aligned} \tag{24}$$

The distribution of C_m is assumed to be diffusive in nature from the starting point. Thus, the GDM for C_m can be noted as

$$\frac{\partial C_m}{\partial t} = \sum_{i=1}^{\infty} K_i(t)\frac{\partial^i C_m}{\partial z_1^i}. \tag{25}$$

According to Gill and Sankarasubramanian [4], the second terms of Eq. (25) describe the diffusive coefficient K_2 of the mean concentration C_m along the z_1 axis respectively. Eq. (25) is then substituted into Eq. (24) and rearranged into the following expression

$$\begin{aligned}&\sum_{i=1}^{\infty} K_i(t)\frac{\partial^i C_m}{\partial z_1^i} + (w - w_m)\frac{\partial C_m}{\partial z_1} - \frac{1}{Pe^2}\frac{\partial^2 C_m}{\partial z_1^2} + \sum_{j=1}^{\infty}\left[\left(\frac{\partial f_j}{\partial t} - L^2 f_j\right)\frac{\partial^j C_m}{\partial z_1^j}\right.\\ &\left.+(w - w_m) f_j \frac{\partial^{j+1} C_m}{\partial z_1^{j+1}} - \frac{1}{Pe^2} f_j \frac{\partial^{j+2} C_m}{\partial z_1^{j+2}} + f_j \sum_{i=1}^{\infty} K_i(t)\frac{\partial^{i+j} C_m}{\partial z_1^{i+j}}\right] = 0.\end{aligned} \tag{26}$$

The diffusion coefficient is obtained by equating the coefficients for the term $\partial^j C_m / \partial z_1^j$ for $j = 1, 2, 3, \ldots,$ and a differential equation of K_2 is obtained as

$$K_2(t) - \frac{1}{Pe^2} + (w - w_m) f_1 + f_1 K_1(t) + \left(\frac{\partial f_2}{\partial t} - L^2 f_2\right) = 0. \tag{27}$$

From Eqs. (22) and (23), the following solvability condition is obtained

$$\int_{k}^{R(z)} f_j r \; dr = 0, \;\; \text{for} \;\; j = 1,2, \ldots, \tag{28}$$

since C_m can satisfy the initial condition of $C.K_2$ in Eq. (27) are then multiplied with r and integrated from the limit k to $R(z)$. Using the solvability condition in Eq. (28), the solution of K_2 is simplified as

$$K_2 = \frac{1}{Pe^2} - \frac{2}{R(z)^2 - k^2} \int_{k}^{R(z)} f_1 w r \; dr. \tag{29}$$

Using Eq. (27), the following set of equations are obtained:

$$\frac{1}{r}\frac{\partial}{\partial r}\left(r\frac{\partial f_{1s}}{\partial r}\right) = (w - w_m), \tag{30}$$

$$\frac{\partial f_{1t}}{\partial t} = \frac{1}{r}\frac{\partial}{\partial r}\left(r\frac{\partial f_{1t}}{\partial r}\right) \tag{31}$$

to solve for the dispersion function f_1 where $f_1(r,t) = f_{1s}(r) + f_{1t}(r,t)$ and f_{1s} is the steady state solution and f_{1t} is the time-dependent part of the solution. Eq. (30) are numerically solved by utilizing the Simpson's 3/8 rule to integrate with respect to r for obtaining the solution of the steady function f_{1s}. For the solution of f_{1t}, separation of variable method is used to solve for Eq. (31) to obtain

$$f_{1t} = \sum_{m=1}^{\infty} A_m B_0(\alpha_m r) e^{-\alpha_m^2 t}, \tag{32}$$

where $B_0(\alpha_m r) = J_1(\alpha_m k) Y_0(\alpha_m r) - Y_1(\alpha_m k) J_0(\alpha_m r)$ and

$$A_m = -\frac{\int_k^{R(z)} f_{1s} B_0 r \; dr}{\int_k^{R(z)} B_0^2 r \; dr}. \tag{33}$$

The factor α_m is the root to equation $Y_1(\alpha_m R(z)) J_1(\alpha_m k) - Y_1(\alpha_m k) J_1(\alpha_m R(z)) = 0$, where J_0, J_1 and Y_0, Y_1 are the Bessel functions of first and second kind respectively, with zero and first order respectively. The obtained dispersion function is then substituted into Eq. (29) to solve for K_2.

2.4 Solution for Mean Concentration

The higher order of $K_i(t)$ starting from $K_3(t)$ is neglected to obtain the generalized dispersion model from Eq. (22) in the form of

$$C(r,z_1,t) = C_m(z_1,t) + f_1(r,t)\frac{\partial C_m(z_1,t)}{\partial z_1}. \tag{34}$$

The mean concentration in Eq. (25) satisfying conditions in Eqs. (18) and (19) resulted in the solution of

$$C_m(z_1,t) = -\frac{1}{2}\left[erf\left(\frac{z_1-\frac{z_s}{2}}{2\sqrt{\omega}}\right) - erf\left(\frac{z_1+\frac{z_s}{2}}{2\sqrt{\omega}}\right)\right], \tag{35}$$

where $\omega = \int_0^t K_2(t)\,dt.$

3. Results and Discussion

The influence of catheter radius and stenosis height on the diffusion coefficient and mean concentration are discussed in this present research. Thus, those parameters are varied such as $k = 0.1, 0.2, 0.3$ and $\delta = 0, 0.1, 0.2$ to observe the graphical trend when the catheter radius and stenosis height increases in a steady manner. Other parameters are chosen to have a constant value appropriately. The power-law index value selected for this study is $n = 0.95$ due to the fact that the common blood flow power-law index values usually lies between $0.9-1.1$ and the typical value of $m = 0.95$ is suitable for $m < 1$ [16]. According to Nagarani and Sebastian [7], the yield stress range of $0-0.1$ and solute length values of 0.02 and 0.004 are within the typical ranges in the cardiovascular system. Thus, the constant for yield stress and solute length are chosen as $\theta = 0.1$ and $z_s = 0.004$ respectively. The graphs plotted are analysed accordingly.

3.1 Diffusion Coefficient

The catheter radius influence on the diffusion coefficient is investigated in Figure 2. Figure 2 shows a decrease in the diffusion coefficient as the catheter radius rises from 0.1 to 0.3. This is because the decrease in the artery flow region that reduces the effectiveness of the diffusion process. When the flow region is small, many blood cells and solutes clustered inside the artery due to the lack of space for diffusion to occur smoothly. Not to mention, for all the catheter radius, the diffusion coefficient increases as the time increases until it reaches a steady diffusion. Significantly, as the time increases, the graphical trend of the diffusion coefficient increment is more inclined when $k = 0.1$ compared to $k = 0.3$. This indicates a rapid diffusion at the beginning of the process when the catheter radius is smaller. Meanwhile, bigger catheter has slower increase in diffusion at the beginning. Another notable dispersion behaviour is the difference in diffusion coefficient values between $k = 0.1$ and $k = 0.2$ is significantly larger compared to the difference in diffusion coefficient values between $k = 0.2$ and $k = 0.3$. Although the increment in catheter radius is in a fixed interval of 0.1, the decrease in diffusion coefficient as the catheter radius increases is substantially different between catheter radiuses.

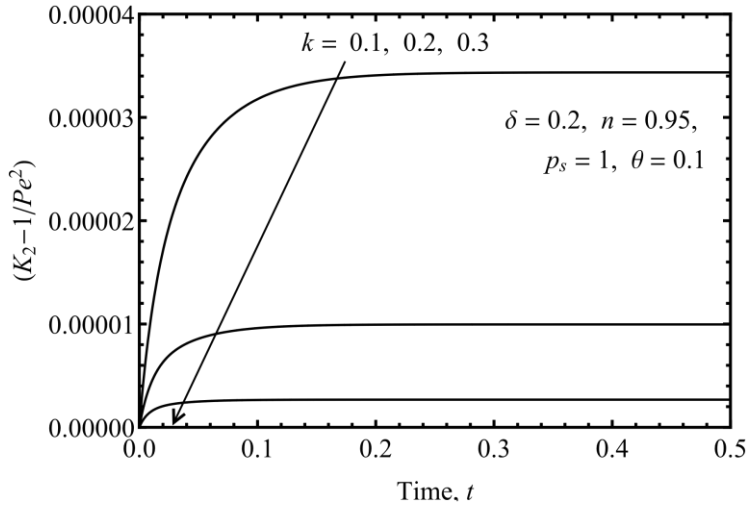

Fig. 2. Diffusion coefficient for varied catheter radius of $k = 0.1, 0.2, 0.3$ with $\delta = 0.2,\ n = 0.95,\ p_s = 1,\ \theta = 0.1$

The effect of stenosis height on the diffusion coefficient is observed in Figure 3. Similarly, the graph shows a decrease in the diffusion coefficient when the stenosis height grows from 0 to 0.2. This is also because of the decrease in the flow region which leads to the solute particles unable to diffuse smoothly. As the time increases, the diffusion coefficient increases until it reaches a constant diffusion. The diffusion at the beginning of the process is also faster when $\delta = 0$ in comparison to $\delta = 0.1$ and $\delta = 0.2$. It can be theoretically concluded that the behaviour of the solute dispersion in terms of the diffusion coefficient is identical when either catheter radius or stenosis height is increased; except that the numerical value of the plotted solution is different. Additionally, a distinguished difference in the numerical values can be observed between Figure 2 and Figure 3. As the stenosis height increases in an interval of 0.1 from $\delta = 0$ to $\delta = 0.1$, the difference in diffusion coefficient is almost similar to when the stenosis height grows from $\delta = 0.1$ to $\delta = 0.2$. Meanwhile, for the catheter radius increment as in Figure 3, the difference in diffusion coefficient varies even though the difference in catheter radius is in a similar interval.

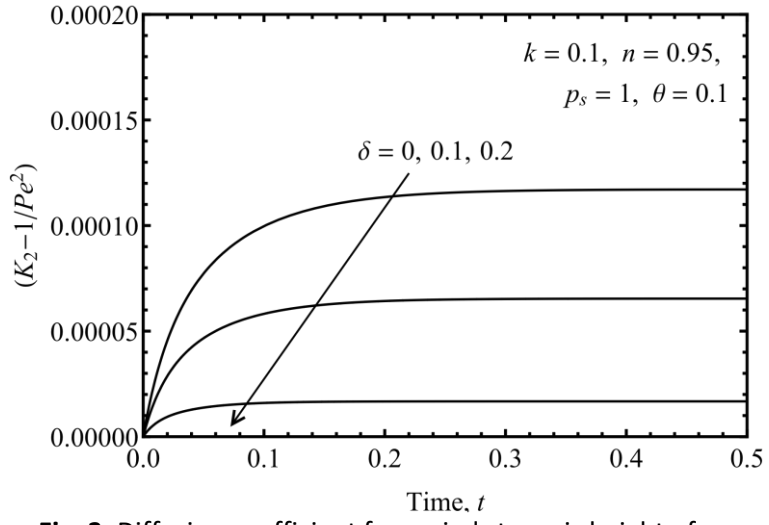

Fig. 3. Diffusion coefficient for varied stenosis height of $\delta = 0, 0.1, 0.2$ with $k = 0.1,\ n = 0.95,\ p_s = 1,\ \theta = 0.1$

3.2 Mean Concentration

Figure 4 is analysed to describe the effect of catheter radius on the mean concentration of solute. Figure 4 shows an increase in the mean concentration as the catheter radius increases from 0.1 to 0.3. The decrease in the flow region caused by the presence of catheter leads to the decrease in diffusion coefficient. As the diffusion process slows down, the solute becomes concentrated at the particular region. This explains the high mean concentration when bigger catheter radius is present within the artery. It can also be observed that the mean concentration increases and decreases between approximately $t=13$ and $t=17$ and peaked at the middle of the mentioned time range for $k=0.1$, where the peak indicates the highest therapeutic level and the effective time for drug dispersion process. However, as the catheter radius increases, the time range for which the mean concentration increases and decreases becomes smaller. Not to mention, as the catheter radius increases, the increase and decay of the mean concentration also becomes rapid as opposed to the slower increase and decreases of mean concentration at smaller catheter radius of $k=0.1$. Another thing to consider, at the time of the highest mean concentration for all catheter radius, the diffusion coefficient is already at a constant diffusion since the diffusion coefficient is already steady starting from $t=0.5$ as shown in Figure 2. However, the mean concentration only occurs after approximately $t=13$.

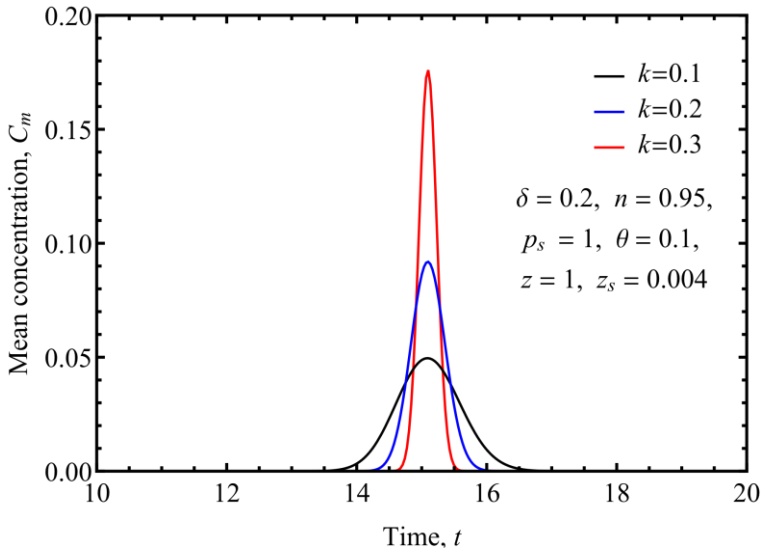

Fig. 4. Mean concentration for varied catheter radius of $k=0.1,0.2,0.3$ with $\delta=0.2$, $n=0.95$, $p_s=1$, $\theta=0.1$, $z=1$, $z_s=0.004$

Figure 5 illustrates the influence of stenosis height on the mean concentration of solute. Figure 5 shows an increment in the mean concentration as the stenosis height grows from 0 to 0.2. The increasing stenosis also decreases the flow region and causes the diffusion process to weaken. The slow diffusion prompts an increase in solute concentration at the particular region. The behaviour of solute dispersion as the stenosis height increases displays a similar trend to when the catheter radius is increased as shown in Figure 4; such that the time range for which the mean concentration increases and decreases becomes smaller as the stenosis height increases. Additionally, the increase and decay of the mean concentration also becomes fast as the stenosis height increases. Nevertheless, a substantial difference of the mean concentration between $\delta=0$ and $\delta=0.1$ and between $\delta=0.1$ and $\delta=0.2$ are highly pronounced. The mean concentration difference between

$\delta = 0.1$ and $\delta = 0.2$ is larger in comparison to the difference between $\delta = 0$ and $\delta = 0.1$. It can also be noted that the mean concentration peaked between the time range of approximately $t = 12.5$ and $t = 18$ for $\delta = 0.1$. Increase in the stenosis height increases the mean concentration peak and reduces the time range in which the peak occurs.

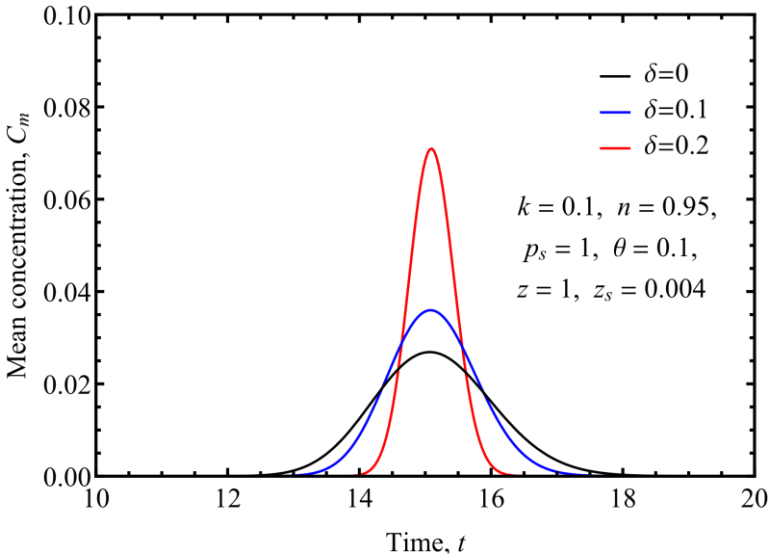

Fig. 5. Mean concentration for varied stenosis height of $\delta = 0, 0.1, 0.2$ with $k = 0.1$, $n = 0.95$, $p_s = 1$, $\theta = 0.1$, $z = 1$, $z_s = 0.004$

Figures 6 (a) and (b) displays the variation of mean concentration against the axial distance under the influence of different catheter radius and stenosis height. Figure 6 (a) shows varying mean concentration when $k = 0.1$ and $\delta = 0$; where the stenosis is absent at $t = 0.2, 0.5, 1.0, 1.5$. It is noted that the highest value of mean concentration for all time is the highest at $t = 0.2$ and lowest at $t = 1.5$. Thus, it can be concluded that the peak mean concentration decreases as the time increases. This is because the solute particles becomes lesser due to the dispersion process that diffuses the solute particles to other region within the artery after some time. It is also noticable that the increase and decrease of the mean concentration is faster at $t = 0.2$ compared to $t = 1.5$. In terms of the axial distance, the location of the mean concentration increases axially as the time increases. Figure 6 (b) illustrates the varying mean concentration when $k = 0.1$ and $\delta = 0.1$; where the stenosis is present at $t = 0.2, 0.5, 1.0, 1.5$. The presence of stenosis reduces the flow region within the artery; therefore decreasing the diffusion coefficient and increasing the mean concentration. This explains the higher numerical value of mean concentration when both catheter and stenosis are present for all time as shown in Figure 6 (b) compared to the mean concentration value when only the catheter is present as shown in Figure 6 (a). Nevertheless, the difference in axial distance between graphs in Figures (a) and (b) at similar time parameters are small.

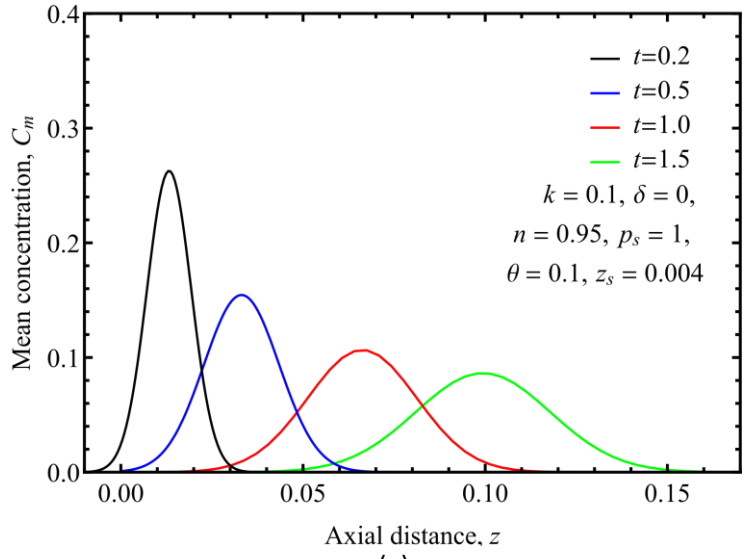

(a)

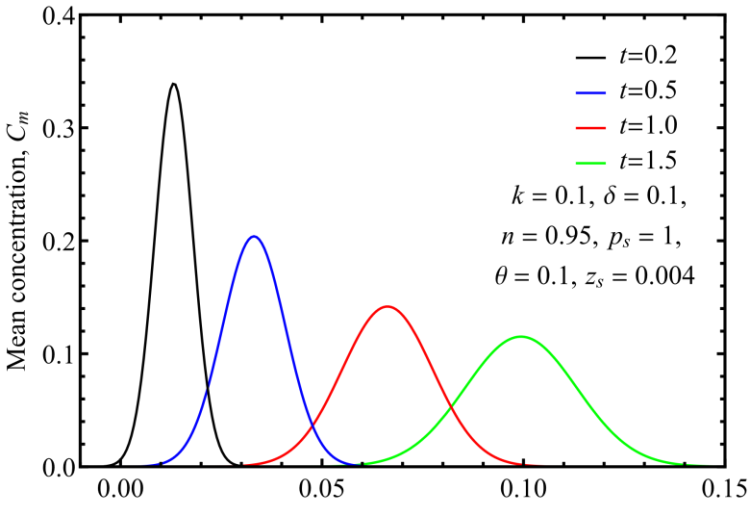

(b)

Fig. 6. Mean concentration for varied time of $t = 0.2, 0.5, 1.0, 1.5$ with $n = 0.95$, $p_s = 1$, $\theta = 0.1$, $z_s = 0.004$ and varied catheter radius and stenosis height of (a) $k = 0.1$ and $\delta = 0$ (b) $k = 0.1$ and $\delta = 0.1$.

4. Conclusion

The present research explores the unsteady solute dispersion in blood flow using the Herschel-Bulkley model through a catheterized stenosed artery. The blood is depicted by the Herschel-Bulkley model. The catheter radius, stenosis height and time parameter effects on the diffusion coefficient and mean concentration are investigated. For the diffusion coefficient, the results show a decrease in the solute diffusion coefficient as either of the catheter radius or stenosis height increases respectively. Nevertheless, for all the catheter radius and stenosis height, the diffusion coefficient increases at the beginning of the process and reaches a constant state as the time parameter increases. However, the rate of diffusion coefficient increment at the beginning depends on either the catheter radius or stenosis height. The smaller the catheter radius or stenosis height, the faster the rate of diffusion coefficient increment. As the increment in catheter radius or stenosis height

leads to the reduction of diffusion coefficient, the mean concentration increases. The reduced diffusion makes the solute particles accumulate at the particular region. Thus, increasing the mean concentration. Nonetheless, the mean concentration decreases as the time increases due to the diffusion process occurring after some time even though in a slower pace. The mean concentration axial distance also increases as the time increases.

From the results obtained, the theoretical aspect of the observations can be applied to the real-life setting. For instance, patients with higher stenosis height in the artery is advised for a smaller catheter radius to ensure the drug solute diffuses efficiently within the flow region space. However, if the intention of the treatment is to accumulate the drug solute within a targeted region, bigger catheter radius should be used. This is because the smaller flow region due to the increased catheter radius will increase the mean concentration at the targeted region. Nevertheless, as the time increases, the diffusion coefficient reaches a constant rate. Therefore, doctors should carefully calculate the safe drug dosage for the time the diffusion is at a constant diffusion rate to optimize the effectiveness of the drug. The mean concentration also decreases and moves further axially within the artery as the time increases. Thus, if the drug solute is supposed to target a local region within the artery, doctors should expect the drug concentration to reduce and moves along the artery after a certain time when calculating the dosage.

This present research opens many possibilities for future studies to be explored. The present research can be further extended to research the solute dispersion in a flow represented by other non-Newtonian models such as Jeffrey, Carreau–Yasuda and many more. One of the areas that can demonstrate the conventional drug delivery system in the biomedical engineering is the nanotechnology field [20]. Nanofluid has gain a reputation in the study of boundary layer flow of thermal convection and concentration diffusion through various setting such as channel flow, pipe flow, stretching sheet and many more. Several types of nanofluid that has been studied for the boundary layer flow is the SWCNT-MWCNT hybrid nanofluid [21], Jefferey nanofluid [22], Al2O3/Water nanofluid [23] and other more. This present research may be further studied by using the nanofluid in representing the blood rheology. Expectantly, this present research and the suggested research problems may motivate other researchers to conduct future studies that contribute to the understanding of the solute dispersion process in blood flow.

Acknowledgement
This research was funded by a grant from Ministry of Education (MOE) through Fundamental Research Grant Scheme (FRGS/1/2020/STG06/UTM/02/15) and also carried up under the research grant GUP Tier 2 (Vote number Q.J130000.2654.17J12).

References

[1] ZainulAbidin, Siti Nurulaifa Mohd, Zuhaila Ismail, and Nurul Aini Jaafar. "Mathematical Modeling of Unsteady Solute Dispersion in Bingham Fluid Model of Blood Flow Through an Overlapping Stenosed Artery." *Journal of Advanced Research in Fluid Mechanics and Thermal Sciences* 87, no. 3 (2021): 134-147. https://doi.org/10.37934/arfmts.87.3.134147

[2] Feltes, Timothy F., Emile Bacha, Robert H. Beekman III, John P. Cheatham, Jeffrey A. Feinstein, Antoinette S. Gomes, Ziyad M. Hijazi et al. "Indications for cardiac catheterization and intervention in pediatric cardiac disease: a scientific statement from the American Heart Association." *Circulation* 123, no. 22 (2011): 2607-2652. https://doi.org/10.1161/CIR.0b013e31821b1f10

[3] Debnath, Sudip, Apu Kumar Saha, B. S. Mazumder, and Ashis Kumar Roy. "Transport of a reactive solute in a pulsatile non-Newtonian liquid flowing through an annular pipe." *Journal of Engineering Mathematics* 116, no. 1 (2019): 1-22. https://doi.org/10.1007/s10665-019-09999-1

[4] Gill, W. N., and R. Sankarasubramanian. "Exact analysis of unsteady convective diffusion." *Proceedings of the Royal Society of London. A. Mathematical and Physical Sciences* 316, no. 1526 (1970): 341-350. https://doi.org/10.1098/rspa.1970.0083
[5] Sebastian, Binil Thomas, and P. Nagarani. "Convection-diffusion in unsteady non-Newtonian fluid flow in an annulus with wall absorption." *Korea-Australia rheology journal* 30, no. 4 (2018): 261-271. https://doi.org/10.1007/s13367-018-0025-7
[6] Nagarani, P., G. Sarojamma, and G. Jayaraman. "Effect of boundary absorption on dispersion in Casson fluid flow in an annulus: application to catheterized artery." *Acta Mechanica* 202, no. 1 (2009): 47-63. https://doi.org/10.1007/s00707-008-0013-y
[7] Nagarani, P., and B. T. Sebastian. "Effect of flow unsteadiness on dispersion in non-Newtonian fluid in an annulus." *Journal of applied mathematics & informatics* 35, no. 3_4 (2017): 241-260. https://doi.org/10.14317/jami.2017.241
[8] Ratchagar, Nirmala P., and R. VijayaKumar. "Dispersion of solute with chemical reaction in blood flow." *Bulletin of Pure and Applied Sciences-Mathematics and Statistics* 38, no. 1 (2019): 385-395. https://doi.org/10.5958/2320-3226.2019.00042.0
[9] Vajravelu, Kuppalapalle, Sreedharamalle Sreenadh, Palluru Devaki, and Kerehalli Prasad. "Mathematical model for a Herschel-Bulkley fluid flow in an elastic tube." *Open Physics* 9, no. 5 (2011): 1357-1365. https://doi.org/10.2478/s11534-011-0034-3
[10] Venkatesan, Jayavelu, D. S. Sankar, K. Hemalatha, and Yazariah Yatim. "Mathematical analysis of Casson fluid model for blood rheology in stenosed narrow arteries." *Journal of Applied Mathematics* 2013 (2013). https://doi.org/10.1155/2013/583809
[11] Rajashekhar, C., G. Manjunatha, K. V. Prasad, B. B. Divya, and Hanumesh Vaidya. "Peristaltic transport of two-layered blood flow using Herschel–Bulkley Model." *Cogent Engineering* 5, no. 1 (2018): 1495592. https://doi.org/10.1080/23311916.2018.1495592
[12] Sankar, D. S., and K. Hemalatha. "Pulsatile flow of Herschel–Bulkley fluid through catheterized arteries–A mathematical model." *Applied Mathematical Modelling* 31, no. 8 (2007): 1497-1517. https://doi.org/10.1016/j.apm.2006.04.012
[13] Sankar, D. S., and Usik Lee. "Two-fluid Herschel-Bulkley model for blood flow in catheterized arteries." *Journal of Mechanical science and technology* 22, no. 5 (2008): 1008-1018. https://doi.org/10.1007/s12206-008-0123-4
[14] Neeraja, G., P. A. Dinesh, K. Vidya, and C. S. K. Raju. "Peripheral layer viscosity on the stenotic blood vessels for Herschel-Bulkley fluid model." *Informatics in Medicine Unlocked* 9 (2017): 161-165. https://doi.org/10.1016/j.imu.2017.08.004
[15] Abbas, Z., M. S. Shabbir, and N. Ali. "Analysis of rheological properties of Herschel-Bulkley fluid for pulsating flow of blood in ω-shaped stenosed artery." *AIP Advances* 7, no. 10 (2017): 105123. https://doi.org/10.1063/1.5004759
[16] Srivastava, V. P., and Rati Rastogi. "Blood flow through a stenosed catheterized artery: Effects of hematocrit and stenosis shape." *Computers & mathematics with applications* 59, no. 4 (2010): 1377-1385. https://doi.org/10.1016/j.camwa.2009.12.007
[17] Gudekote, Manjunatha, Rajashekhar Choudhari, Hanumesh Vaidya, and Kerehalli Vinayaka Prasad. "Peristaltic flow of Herschel-Bulkley fluid in an elastic tube with slip at porous walls." *Journal of Advanced Research in Fluid Mechanics and Thermal Sciences* 52, no. 1 (2018): 63-75.
[18] Jaafar, Nurul Aini, Siti NurulAifa Mohd ZainulAbidin, Zuhaila Ismail, and Ahmad Qushairi Mohamad. "Mathematical Analysis of Unsteady Solute Dispersion with Chemical Reaction Through a Stenosed Artery." *Journal of Advanced Research in Fluid Mechanics and Thermal Sciences* 86, no. 2 (2021): 56-73. https://doi.org/10.37934/arfmts.86.2.5673
[19] Tey, Wah Yen, Yutaka Asako, Nor Azwadi Che Sidik, and Rui Zher Goh. "Governing equations in computational fluid dynamics: Derivations and a recent review." *Progress in Energy and Environment* 1 (2017): 1-19.
[20] Rathore, Surabhi, and D. Srikanth. "Mathematical study of transport phenomena of blood nanofluid in a diseased artery subject to catheterization." *Indian Journal of Physics* 96, no. 7 (2022): 1929-1942. https://doi.org/10.1007/s12648-021-02166-2
[21] Kumar, T. Prasanna. "Heat Transfer of SWCNT-MWCNT Based Hybrid Nanofluid Boundary Layer Flow with Modified Thermal Conductivity Model." *Journal of Advanced Research in Fluid Mechanics and Thermal Sciences* 92, no. 2 (2022): 13-24. https://doi.org/10.37934/arfmts.92.2.1324
[22] Zokri, Syazwani Mohd, Nur Syamilah Arifin, Abdul Rahman Mohd Kasim, and Mohd Zuki Salleh. "Free convection boundary layer flow of Jeffrey nanofluid on a horizontal circular cylinder with viscous dissipation effect." *Journal of Advanced Research in Micro and Nano Engineering* 1, no. 1 (2020): 1-14.

[23] Elfaghi, Abdulhafid MA, Alhadi A. Abosbaia, Munir FA Alkbir, and Abdoulhdi AB Omran. "CFD Simulation of Forced Convection Heat Transfer Enhancement in Pipe Using Al2O3/Water Nanofluid." *Journal of Advanced Research in Numerical Heat Transfer* 8, no. 1 (2022): 44-49.